Journal of Inorganic and General Chemistry
ZAAC
Zeitschrift für anorganische und allgemeine Chemie
www.zaac.wiley-vch.de
RESEARCH ARTICLE
Check for updates
DOI: 10.1002/zaac.202100389

The Cesium Oxide Mercuride $Cs_{18}Hg_8O_6$

Lukas Nusser,[a] Timotheus Hohl,[a] Frank Tambornino,[b] and Constantin Hoch*[a]

Dedicated to Prof. Dr.-Ing. Caroline Röhr on the Occasion of her 60th Birthday

By reacting Cs with Cs_2O and elemental mercury the new double salt $Cs_{18}Hg_8O_6$ could be obtained. Its crystal structure (cubic, space group $I23$ with $a = 13.3920(10)$ Å, $Z = 2$, $R1 = 0.026/0.032$ for $I \geq 2\sigma(I)$/all I, respectively) comprises isolated oxide anions in octahedral coordination by cesium cations next to the mercuride anion $[Hg_8]^{6-}$. This first isolated anion of mercury has cubic shape and is coordinated by cesium atoms capping the faces and the edges of the $[Hg_8]^{6-}$ cube. The ionic character of the double salt is shown in DFT calculations of the electronic structure. Raman spectra show distinct features in the low energy region arising from the vibrations of the mercuride anion. $Cs_{18}Hg_8O_6$ has very close structural analogies to the thallide oxide $Cs_{18}Tl_8O_6$.

Introduction

Mercury does not form anions that easily. Reacting mercury with the most electropositive elements (Li–Cs, Mg–Ba, La–Lu) results in the formation of highly polar, yet always metallic amalgams.[1] The electron transfer is incomplete in all cases, and negatively polarised Hg atoms or atom groups $[Hg_n]^{\delta-}$ are observed, but no 'true' $[Hg_n]^{m-}$ anions. This may be related to the fact that mercury does not form a stable atomic anion in the gas phase,[2] according to its closed-shell configuration $4f^{14}5d^{10}6s^26p^0$, in contrast to other noble metals and its neighbouring elements Pt, Au, Tl and Pb.

Double salts containing oxide and metalide anions simultaneously are numerous and have a long history. In the utmost cases, the metalide anions in these double salts are thermodynamically stable Zintl anions derived from highly electronegative elements, and the double salt structures profit from optimisation of local Coulombic fields. First and prominent members of this family are the anti-Perovskite structures A_3MO with $A = Ca^{2+}$, Sr^{2+}, Ba^{2+} and $M = Sn^{4-}$, Pb^{4-}.[3] This series has since then been extended by members with $A = Eu$ and other lanthanoids, $M = Si$, Ge, P, As, Sb, Bi, Zn, Ga, Au, and also for B^{3-}, C^{4-}, N^{3-} instead of O^{2-}.[4] These anti-Perovskite materials have found a great resonance in physical materials sciences due to their electric properties until today.[5]

Double salts combining oxide anions with a variety of Zintl anions have been studied over the last decades.[6] This class of double salts has further been extended with compounds containing Zintl anions and oxometalate anions $[MO_x]^{y-}$ instead of isolated oxide anions. This is interesting especially in those cases where the metal in the metalide anion and the oxometalate anion is the same because then the compounds are thermodynamically unstable with regard to the comproportionation reaction of the element M existing in a negative and a positive oxidation state. Within this context, tetrelide tetrelates[7] and also auride aurates[8] have been studied. Nitridic germanide germanates have also been described,[9] with the formal oxidation states of germanium spanning the maximum range from Ge^{4-} to Ge^{4+} in one example.

The only literature examples for double salts with oxide anions and metalide anions which do not represent classical Zintl anions are several alkali metal oxide thallides:[10] Thereof namely $Cs_{18}Tl_8O_6$[10c,d,e] is of high interest for this study as it has the same stoichiometric composition as the title compound and the very close structural relationships will require a detailed comparative discussion. Here we report on synthesis, crystal structure, Raman spectroscopy and aspects of the chemical bonding in the cesium oxide mercuride, $Cs_{18}Hg_8O_6$ containing the first isolated mercuride anions $[Hg_8]^{6-}$.

Results and Discussion

Single crystal structure description: $Cs_{18}Hg_8O_6$ crystallises in a cubic structure with space group $I23$, see Table 1 for basic crystallographic data, Table 2 for atomic coordinates, Table 3 for coefficients of the anisotropic displacement parameter and Table 4 for selected interatomic distances. Its structure is closely

[a] L. Nusser, T. Hohl, C. Hoch
Department Chemie
Ludwig-Maximilians-Universität München
Butenandtstr. 5–13, Haus D
81377 München
Germany
Fax: +49 (0)89 2180-77440
E-mail: constantin.hoch@cup.uni-muenchen.de
[b] F. Tambornino
Fachbereich Chemie
Phillips-Universität Marburg und Wissenschaftliches Zentrum für Materialwissenschaften (MZMW)
Hans-Meerwein-Straße 4
35032 Marburg
Germany

Table 1. Crystallographic data and details on data collection, structure solution and refinement of $Cs_{18}Hg_8O_6$ at 293 K.

Empirical sum formula	$Cs_{18}Hg_8O_6$
Crystal system	cubic
Space group	*I*23 (No. 197)
Lattice parameters (Å, Å^3)	$a = 13.3920(10)$ $V = 2401.8(5)$
Formula units Z	2
Calculated density (g cm^{-3})	5.66
Absorption coefficient (mm^{-1})	38.92
Radiation, wavelength (Å)	MoK_α, 0.71073
Diffractometer	Bruker D8 Quest
Corrections	Lorentz, polarisation, absorption (indexed crystal faces)[14]
Number of l.s. parameters	28
Number of collected data	30450
Number of unique data	1173
unique data with $I \geq 2\sigma(I)$	1131
R_{int}/R (σ)	0.0790/0.0514
Indexing range	$-18 \leq h, k, l \leq 18$
Data range (°)	$6.0 \leq 2\vartheta \leq 60.0$
Structure solution	Direct methods[14]
Structure refinement	Full matrix least-squares on F^2[14]
Final R values [$I \geq 2\sigma(I)$]	$R1 = 0.0260$ $wR2 = 0.0446$
Final R values (all data)	$R1 = 0.0312$ $wR2 = 0.0452$
Goodness of Fit	1.075
Res. e$^-$ density min/max (e$^-$ Å^{-3})	$-1.26/+2.14$
CCDC deposition number	2130332

related to the $Cs_{18}Tl_8O_6$ structure (see next paragraph). The crystal structure of $Cs_{18}Hg_8O_6$ is shown in Figure 1 and contains two different types of anions, both coordinated by cesium cations. The cesium atoms occupy two crystallographically independent sites and are both in contact with the oxide and the mercuride anions. The single crystallographic oxide ion position shows distorted octahedral coordination by cesium cations as is common in many ionic oxidic compounds. The connection pattern of the $[Cs_6O]$ units via common edges leads to a Cs–O network in which the $[Hg_8]^{6-}$ anions are embedded. Coordination geometry as well as interatomic Cs–O distances (see Table 4) show no significant deviations from the geometric details for oxide anions coordinated by cesium cations in Cs_2O or Cs_2HgO_2, the only known cesium oxomercurate[11] (d_{Cs-O} in Cs_2O: 286.3[11b] to 292.1 pm,[11a] in Cs_2HgO_2: 309.1 pm). In all cases a slightly distorted octahedral coordination $[Cs_6O]$ is realised. The mercuride anion is composed of two crystallographically independent Hg sites with identical Wyckoff letter 8*c*. They form a slightly distorted cube (see Table 4, maximum deviation of the interatomic angles from 90°: 5.26(2)°, Hg–Hg distances equal within error margin). The Hg–Hg distances with 295 pm are very close to those found for Hg atoms in mercury-rich amalgams and considerably longer than those found for Hg–Hg contacts in Hg^+ compounds like Hg_2Cl_2 (259.5 pm[12]). The only comparable $[Hg_8]$ unit can be found in the crystal structure of $Rb_{15}Hg_{16}$,[13d] and also here the structural deviations from an ideal cube are marginal (d_{Hg-Hg} ranging from 293.9 to 297.9 pm, largest deviation from 90° for the Hg–Hg–Hg angles: ±4.34°). $[Hg_4]$ squares appear more commonly in the crystal structures of the amalgams $Rb_{15}Hg_{16}$, KHg, CsHg and Na_3Hg_2.[13] Again, Hg–Hg distances in the same range (295 to 302 pm) are observed and the deviations from 90° for the Hg–Hg–Hg angles are found even smaller (typically ±0.3–0.7°). The topology of the packing of the building units of the crystal structure can be rationalised by describing the cesium-coordinated Hg entity $[Cs_{18}Hg_8]$ as a quasi-spherical unit (see Figure 1, lower right). The packing of these spheres follows a bcc pattern embedded in β cages built from oxide anions.

Comparison with the structure of $Cs_{18}Tl_8O_6$: The crystal structure of $Cs_{18}Tl_8O_6$ is very closely related to the one of $Cs_{18}Hg_8O_6$. Both crystallise in the same space group type with occupation of the same number of sites with equal Wyckoff letters. Both structures thus are isopointal and the crystallo-

Table 2. Standardised[14] fractional atomic coordinates and equivalent isotropic displacement parameters (Å^2) for $Cs_{18}Hg_8O_6$. U_{eq} is defined as 1/3 of the trace of the orthogonalised U_{ij} tensor. Standard deviations in units of the last digit are given in parentheses.

Atom	*x*	*y*	*z*	Wyckoff site	U_{equiv}
Cs1	0.04517(8)	0.32662(5)	0.28613(5)	24*f*	0.0526(3)
Cs2	0.36496(6)	0	0	12*d*	0.0513(3)
Hg1	0.10500(3)	*x*	*x*	8*c*	0.0359(2)
Hg2	0.38461(3)	*x*	*x*	8*c*	0.0390(2)
O1	0.3255(7)	$^1/_2$	0	12*e*	0.034(2)

Table 3. Coefficients U_{ij} (Å^2) of the anisotropic atomic displacement parameters for $Cs_{18}Hg_8O_6$. U_{ij} is defined as $\exp\{-2\pi^2[U_{11}(ha^*)^2 + \ldots + 2\,U_{12}hka^*b^*]\}$. Standard deviations in units of the last digit are given in parentheses.

Atom	U_{11}	U_{22}	U_{33}	U_{23}	U_{13}	U_{12}
Cs1	0.0922(6)	0.0356(4)	0.0300(3)	0.0007(3)	0.0067(3)	0.0106(4)
Cs2	0.0272(4)	0.0326(4)	0.0940(8)	0.0075(5)	0	0
Hg1	0.0359(2)	U_{11}	U_{11}	−0.0005(2)	U_{23}	U_{23}
Hg2	0.0390(2)	U_{11}	U_{11}	0.0027(2)	U_{23}	U_{23}
O1	0.037(5)	0.040(5)	0.026(4)	0.004(5)	0	0

Table 4. Selected interatomic distances (pm) and angles (°) and their frequencies for $Cs_{18}Hg_8O_6$. Standard deviations in units of the last digit are given in parentheses.

Atoms		*d*	Atoms			∠
Hg1 –	Hg2	295.80(6) (3x)	Hg2	– Hg1 –	Hg2	95.26(2) (3x)
	Hg2	295.81(6) (3x)	Hg1	– Hg2 –	Hg1	84.49(2) (3x)
Cs1 –	Hg1	391.31(8)	Cs1	– O1 –	Cs1	87.88(9) (2x)
	Hg2	422.54(10)	Cs1	– O1 –	Cs1	92.43(19) (2x)
Cs2 –	Hg1	400.93(8)	Cs1	– O1 –	Cs1	116.1(3)
	Hg2	399.33(8)	Cs1	– O1 –	Cs1	179.4(4)
O1 –	Cs1	282.7(5) (2x)	Cs1	– O1 –	Cs2	82.5(1) (2x)
	Cs1	292.74(7) (2x)	Cs1	– O1 –	Cs2	85.15(5) (2x)
	Cs2	295.5(7) (2x)	Cs1	– O1 –	Cs2	97.0(2) (2x)
			Cs2	– O1 –	Cs2	157.1(2) (2x)
			Cs2	– O1 –	Cs2	75.5(2)

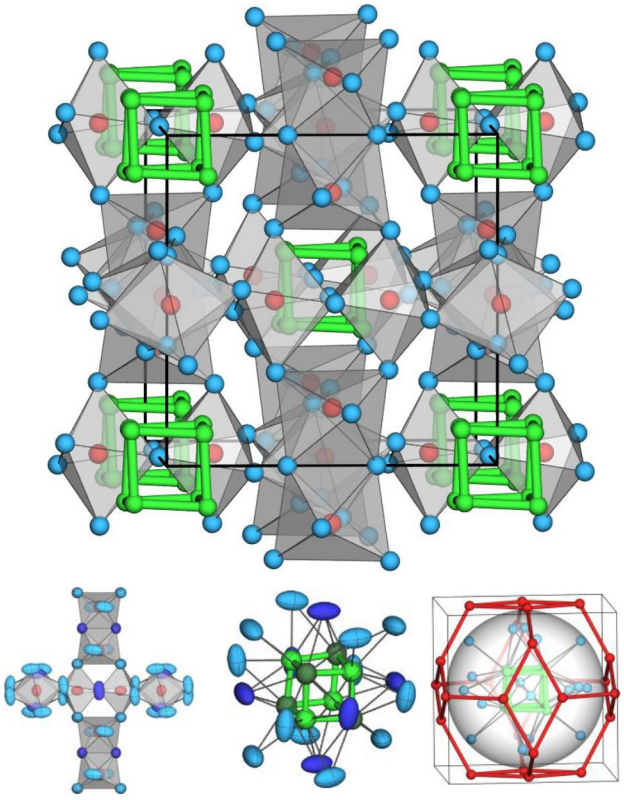

Figure 1. Above: Extended unit cell of $Cs_{18}Hg_8O_6$ in a projection approximately along *a*. Green cubes depict the $[Hg_8]^{6-}$ anions, oxide anions are drawn as red spheres, cesium cations as blue spheres. $[Cs_6O]$ coordination polyhedra are shown as grey transparent octahedra. The unit cell axes are shown in black. Lower left: connection pattern of the coordination polyhedra of cesium cations around oxide anions in $Cs_{18}Hg_8O_6$. Viewing direction is along *a*. Cs1 atoms are drawn in light blue, Cs2 atoms in dark blue. All atoms are drawn as ellipsoids on a probability level of 99%. Lower center: $[Hg_8]^{6-}$ anion in $Cs_{18}Hg_8O_6$ and its coordination by Cs cations in a general viewing direction. Hg1 atoms are drawn in light green, Hg2 atoms in dark green, Cs1 atoms are shown in light blue and Cs2 atoms in dark blue. Cs1 atoms cap all edges of the Hg cube and Cs2 atoms cap the faces. Lower right: $[\mu2\text{-}Cs1_{12}\mu3\text{-}Cs2_6Hg_8]^{12+}$ embedded in the $[O_{24/4}]^{12-}$ β cage. The radius of the grey sphere is defined by the longest Cs–Hg distance to 6.25 Å. Ellipsoids are drawn on a probability level of 99% for all atoms.

graphic configurations (crystallographic orbits) are similar to a certain degree. A graphical juxtaposition of both structures is shown in Figure 2. Geometric deviations, lattice distortion and the value Δ as the standardised measure of similarity[15] are given in Table 5. The orbits of both Tl/Hg atomic positions with Wyckoff letter 8*c* differ significantly. In the case of the Hg compound, the two orbits result in the formation of cubic $[Hg_8]^{6-}$ units whereas in the case of the Tl compound the orbits form a $[Tl_{4+4}]^{6-}$ stellated tetrahedron. The coordination of these metalide building units by cesium atoms consequently has to adjust but shifts in the Cs atomic positions are only marginal.

It becomes clear that $Cs_{18}Tl_8O_6$ and $Cs_{18}Hg_8O_6$ are very closely related structures, and based only on the small value Δ it would be reasonable to call them isotypic. Due to the considerable local structural differences between the two metalide anions, however, we suggest to address the two structures as being homeotypic.

Calculation of the electronic structure: The calculated Density of States (DOS, see Figure 3) shows several discrete features. A small but distinct band gap at the Fermi level indicates non-metallic behaviour and justifies the picture of a double salt. All oxide-centered p states are located in a narrow energy range between −1.9 and −1.1 eV. The small dispersion of the three levels slightly differing in their relative energies reflects the localisation of the p eletrons. Also the bands belonging to the $[Hg_8]^{6-}$ anion show narrow dispersion. The bands directly below the Fermi in the range between 0 and −0.7 eV belong to 3 bands accomodating the 6 p skeletal electrons for the $[Hg_8]^{6-}$ cluster anion. In a simplified picture, this would account for 12 p-p σ bonds along the edges of the $[Hg_8]$ cube with bond order 1/2. The Hg electronic states are well separated from the oxide-centered states by a band gap of ca. 0.4 eV, indicating no significant interaction of the two anionic species and again making the chemical picture of a double salt plausible. In the energy region below −2 eV only Hg s, p and d states with very low dispersion and high degeneracy are visible. They belong to inert electron pairs with mixed sp character and high localisation (−3 to −4.5 eV) and to Hg d states (−6.5 eV and lower) treated as core electrons.

There are striking similarities between the electronic structure reported for $Cs_{18}Tl_8O_6$[10c,d,e] and the one presented

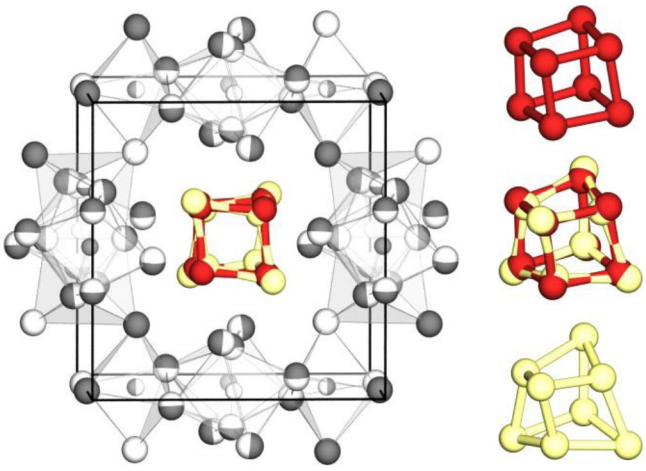

Figure 2. Comparison of the structures of $Cs_{18}Hg_8O_6$ and $Cs_{18}Tl_8O_6$. Left: Overlay of both unit cells. Dark grey atoms belong to the Tl compound, light grey atoms to the Hg compound. Red atoms are Hg, yellow atoms are Tl. Top right: the $[Hg_8]^{6-}$ cube, bottom right: The $[Tl_8]^{6-}$ stellated tetrahedron, center right: their overlay. All atoms are drawn as spheres with arbitrary radii.

Table 5. Geometric comparison of the crystal structures of $Cs_{18}Hg_8O_6$ and $Cs_{18}Tl_8O_6$. Shown are the pairs of corresponding atomic fractional coordinates and their absolute difference |u| in Å. Parameters suitable to evaluate structural similarity are the degree of lattice distortion S, maximum and mean displacement between paired atoms $d_{max.}$ and $d_{av.}$ and the measure of similarity Δ.[15]

$Cs_{18}Hg_8O_6$ $Cs_{18}Tl_8O_6$	Wyck.	*x*	*y*	*z*	|u|/Å
Hg1	8*c*	0.1050	*x*	*x*	0.362
Tl1		0.0894	*x*	*x*	
Hg2	8*c*	0.3846	*x*	*x*	0.441
Tl2		0.3656	*x*	*x*	
Cs1	24*f*	0.0452	0.3266	0.2861	0.088
Cs1		0.0517	0.3260	0.2864	
Cs2	12*d*	0.3650	0	0	0.002
Cs2		0.3648	0	0	
O1	12*e*	0.3255	1/2	1/2	0.020
O1		0.3270	1/2	1/2	
Structure similarity evaluation parameters		S	$d_{max.}$/Å	$d_{av.}$/Å	Δ
		0.0008	0.4408	0.1375	0.015

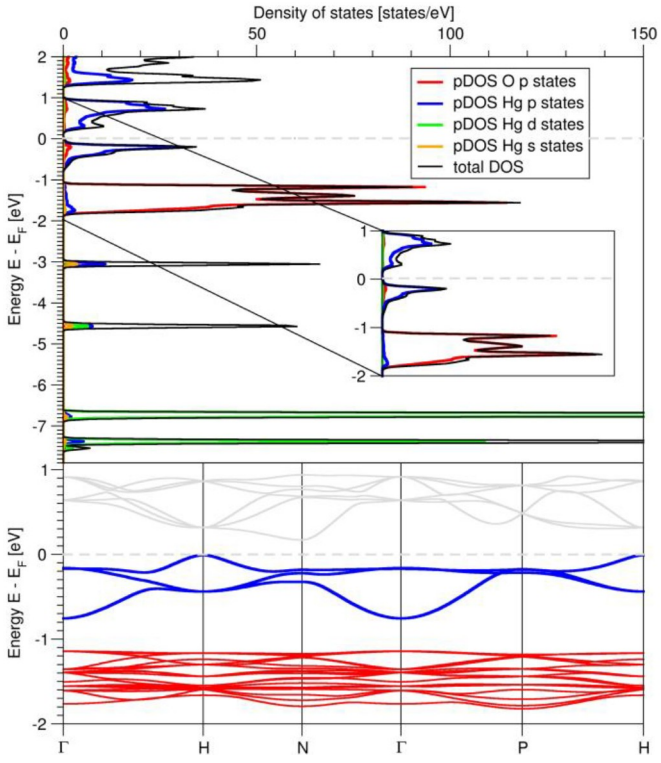

Figure 3. Electronic structure calculations for $Cs_{18}Hg_8O_6$. Above: DOS plots with total DOS in black, partial DOS for O p states in red and for Hg p states in blue, Hg d states in green. The Fermi level is indicated by the grey dashed line. The inset shows the magnified energy range from +1 to −2 eV. Below: spaghetti plots in the energy region close to the Fermi level. Hg p bands are shown in blue, O p bands in red.

here for $Cs_{18}Hg_8O_6$. The difference between them result from the individual electronic situation in the metalide cluster anions. A $[Tl_8]^{6-}$ entity with 8 electrons more in the skeletal orbitals stabilised by the structural distortion described above, and the electronic situation in the $[Hg_8]^{6-}$ anion affords for a different local geometry in order to maximise the energy gap between HOMO and LUMO states. It can be assumed that the 'mercubanide' anion shows a closed-shell and energetically optimised configuration with only marginal deviation from ideal cubic arrangement of the Hg atoms. Detailed calculations with this respect are in progress, also taking into account the spin-orbit coupling contributions. Extended and detailed electronic structure calculations not only on thallide cluster anions[10] but also on aurides and platinides[16] have shown the high importance of taking spin-orbit contributions appropriately into account.

Vibrational spectroscopy: On small crystalline samples of $Cs_{18}Hg_8O_6$ sealed in quartz capillaries Raman spectra were recorded in transmission mode with a Nd laser (λ = 632.817 nm, 1 μm beam size, power 1 mW, 50-fold magnification optics). The spectrum, see Figure 4, shows several distinct features in the low frequency range. The normal frequencies of a $[Hg_8]^{6-}$ species can be expected to occur only at very low wave numbers, however, the exact values remain unknown. Three of the eight normal modes of a cube are Raman-active (A_{1g}, E_g and one of the two F_{2g}).[17] The recorded signal can be grouped into three ranges at 30 cm^{-1}, 44–80 cm^{-1} and 100 cm^{-1}. Splitting of the three normal modes of an ideal cube into multiple signals can be expected due to the distortion of the $[Hg_8]$ unit in $Cs_{18}Hg_8O_6$. The attribution of the observed Raman frequencies to the three Raman-active normal modes of the cubic anion can, however, not be made without comparison with Raman spectra of other $[Hg_8]$-containing compounds or quantum-molecular calculations. Calculations with this respect are an

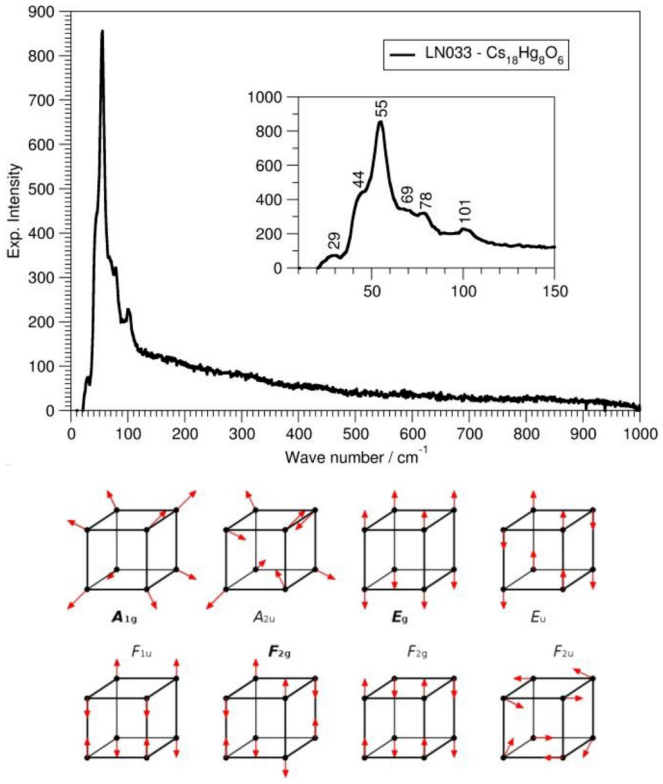

Figure 4. Top: Raman spectrum of $Cs_{18}Hg_8O_6$. Bottom: the eight normal vibration modes of a cube with point group O_h. The three Raman-active modes are emphasised by bold letters.

ongoing project as well as spectroscopic studies on other mercuride oxides.

Stability of mercuride anions in double salts: As stated above, mercury does not form a stable anion in the gas phase. The existence of such anions is quite common, though, within solids. The second electron affinity of oxygen, for example, is highly unfavourable, yet highly ionic oxides are abundant and show in many cases very high thermal and chemical stability. For nitrogen, already the first electron affinity is unfavourable, yet a high and still growing number of ionic nitrides and nitridic solids are known. The anions are stabilised by the lattice energy, comprising the Coulombic local crystal fields and their geometric optimisation in the sense of the second Pauling rule for ionic crystals. There are many highly ionic structures with nonetheless low lattice energy due to inconvenient local atomic arrangement. For example, many '*ortho*' metalates $A_n[MO_4]$ with isolated tetrahedral oxometalate anions $[MO_4]^{n-}$are unknown. In these cases, the insertion of additional, isolated oxide anions can stabilise the lattice – for example, the oxide orthogermanate $Cs_{10}[GeO_4]_2O$ has been described[18], whereas Cs_4GeO_4 is unknown. With this in mind, it can be rationalised that the first 'true' isolated mercuride anion is found in a double salt structure together with isolated oxide anions.

Conclusions

With $Cs_{18}Hg_8O_6$ the existence of isolated mercury anions can be proven. Mercuride anions can be stabilised in double salt structures together with oxide anions by a sufficiently high lattice energy. Rather than isolated monoatomic Hg^- anions a $[Hg_8]^{6-}$ cluster anion is formed. The simple picture of p-p σ interactions with 6 p electrons serving for 12 bonds along the cube edges with bonding order of 1/2 is corroborated by DFT calculations, suggesting the picture of an ionic double salt in which the two anions O^{2-} and $[Hg_8]^{6-}$ do not show significant interactions. The structural building blocks show geometrical details known from either cesium oxides or cesium amalgams. The Raman spectrum shows a quasi-molecular vibration behaviour for the $[Hg_8]^{6-}$ anion.

Future investigations will concentrate on further oxide mercurides containing $[Hg_8]^{6-}$ anions or other multinuclear mercuride anionic units. Calculations of the molecular properties will help in the interpretation of the observed vibrational spectra, and detailed DFT calculations of the crystal structures will reveal deeper insight into the Hg–Hg interactions and the underlying reasons for the stability of (a) cubic anions and (b) the charge of −6 for the cubic anionic units.

The newly discovered mercuride anions represent an interesting 'missing link' in the series of anions of the highly relativistic metals Pt, Au, Hg, Tl and Pb. The anions from elements showing high electron affinities can be rationalised with simple electron counting rules, whereas Tl and also Hg anionic entities show a more complex behaviour. The direct comparability of thallide and mercuride anions in very similar crystal structures on the basis of analysing the cluster units on a local approach will help understanding the correlation of electron count, bonding situation details and their influence on geometric distortions.

Experimental Section

Materials: Cesium metal (distilled) was taken from own production (Max-Planck-Institut für Festkörperforschung, Stuttgart, Germany) or from donations of Kriminalpolizei Heilbronn, Germany. Hg was purified by stirring the raw metal in half-conc. HNO_3, filtration and subsequent multiple distillation. HgO (Sigma Aldrich, p. a.) was used without further purification.

Preparation: $Cs_{18}Hg_8O_6$ was first observed as the main product of the following synthetic procedure. A glass reactor was used consisting of a wide tube with convex bottom and two connection cocks. One connects the reactor to the Schlenk line (vacuum/argon), the other one to a small Schlenk tube filled with HgO. This serves as oxygen source via thermal decomposition. To prevent Hg vapour from entering the reactor, a small cooling trap with ice/NaCl cooling mixture was inserted between the HgO Schlenk tube and the reactor. Inside an argon-filled glove box the reactor was loaded with 2.906 g (21.867 mmol) Cs and 1.269 g (7.324 mmol) Hg. Mixing the two metals results in heating and should be performed with care: it is convenient to add Hg dropwise to Cs and not vice versa. The closed reactor was connected to a Schlenk line and to the HgO Schlenk tube with cooling trap. 1.623 g (7.493 mmol) of HgO were filled into the Schlenk tube. Assuming all HgO to be decomposed into O_2, the reaction mixture in the reactor was calculated to give

the composition Cs_3HgO (6,000 g in total). This composition was found to be of interest in previous experiments resulting in further new compounds containing Hg anions next to oxide anions. They will be the topic of future publications. Prior to the oxidation reaction, the Cs–Hg mixture in the reactor was homogenised by mild heating to ca. 40 °C in an oil bath and stirring with a magnetic stirrer under vacuum ($p \leq 1 \cdot 10^{-3}$ mbar). The evacuated reactor was separated from the Schlenk line (static vacuum) and slow oxygen evolution was started by heating the HgO Schlenk tube with a heat gun until decomposition. The initial golden color of the liquid metallic mixture started to darken with increasing oxygen content, quite as described for the synthesis of cesium suboxides from the elements. At higher oxygen contents, however, a reddish taint started to become perceptible. The reaction mixture had to be heated gradually to a temperature of $T_{max} = 160$ °C in order to stay liquid. After completing the oxygen evolution the mixture was cooled to room temperature and a crystalline black solid with metallic luster was obtained. The reactor was transferred to the glove box. Phase analysis of the product mixture by X-ray powder diffraction (see Figure 5) shows the presence of Cs_3O as byphase next to $Cs_{18}Hg_8O_6$ as the main phase. Additional diffraction maxima with comparatively low intensities point toward the presence of other, new phases suggesting further investigations.

Single crystal and powder diffraction analysis: Portions of the reaction product were transferred from the glove box in a dish covered with paraffin oil dried over potassium. Single crystal specimens suitable for single crystal investigations were selected under a binocular and sealed in oil-filled glass capillaries. The crystals were mounted on the goniometer of a D8 Quest diffractometer system (Bruker AXS, Karlsruhe, Germany) and checked for quality. After establishing the orientation matrix from preliminary frame sets the reflection intensities of 1/2 of the Ewald sphere were collected in combined ω and ϕ scans. After integration the net intensities were corrected for polarisation and Lorentz effects.[14] According to the high absorption coefficient an absorption correction was carefully performed on the basis of indexed crystal faces.[14] Structure solution was peformed with direct methods and revealed the positions of all Cs and Hg atoms. In the course of subsequent full-matrix least-squares refinement cycles, the O atomic position was detected from the difference Fourier synthesis. All atoms were refined with anisotropic treatment of the thermal displacement.

X-ray powder diagrams were recorded on a transmission powder diffractometer (Stoe STADI-P, Stoe, Darmstadt, $MoK_{\alpha 1}$ radiation, germanium monochromator) in Debye-Scherrer geometry on capillary samples. The sample had to be diluted with diamond powder due to its ductility and for optical dilution. The diffraction pattern is shown in Figure 5.

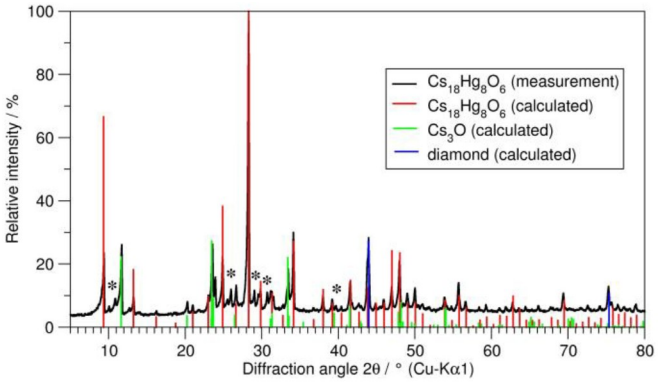

Figure 5. Powder X-ray diffraction pattern of a sample with $Cs_{18}Hg_8O_6$ as the main reaction product and Cs_3O as a a byphase. Reflections which could not be attributed to a known phase are marked with asterisks.

DFT calculations of the electronic band structure were performed with the program suite Wien2K.[19] The full-potential linear augmented plane wave (FP-LAPW) was applied with the exchange and correlation functional with a generalised gradient approximation (GGA-PBE).[19] Muffin-tin radii were set to 250 pm and the number of basis functions was determined by the value of $R_{mt} * K_{max} = 7$ with K_{max} being the largest k vector. The separation energy was set to −6 Ry and a 10×10×10 Monkhorst-Pack grid was applied. Spin-orbit coupling was not explicitly taken into account, relativistic corrections were performed on a merely scalar level.

Acknowledgements

The authors would like to thank Irina Zaytseva for the initial observation leading to this study: The first occurence of a cesium oxide mercuride was caused by Hg contaminations during the Cs_2O preparation process. Jessica Wulfes helped with preparative studies assuring that the observed phase was not a new binary cesium amalgam. The authors are greatly indebted to Armin Schulz, Max-Planck-Institut für Festkörperforschung, Stuttgart, for recording the Raman spectra. We would also like to thank Ulrich Wedig, Max-Planck-Institut für Festkörperforschung, Stuttgart, for fruitful discussions and valuable suggestions. Open Access funding enabled and organized by Projekt DEAL.

Conflict of Interest

The authors declare no conflict of interest.

Data Availability Statement

The data that support the findings of this study are available from the corresponding author upon reasonable request.

Keywords: Double salts · Mercubanide · Structure elucidation · Raman spectroscopy · DFT calculations

[1] a) H. J. Deiseroth, *Prog. Solid State Chem.* **1997**, *25*, 73–123; b) M. Wendorff, C. Röhr, *Z. Kristallogr.* **2018**, *233*, 515–529.
[2] J. H. Simons, R. P. Seward, *J. Chem. Phys.* **1938**, *6*, 790–794.
[3] A. Widera, H. Schäfer, *Mat. Res. Bull.* **1980**, *15*, 1805–1809.
[4] a) E. F. Bertaut, D. Fruchart, J. P. Bouchaud, R. Fruchart, *Solid State Commun.* **1968**, *6*, 251–256; b) D. Fruchart, E. F. Bertaut, R. Mader, R. Fruchart, *J. Phys.* **1971**, *32*, 876–877; c) R. Türck, PhD Thesis **1994**, Universität Stuttgart, Germany; d) C. Feldmann, M. Jansen, *J. Chem. Soc. Chem. Commun.* **1994**, *9*, 1045–1046; e) C. Feldmann, M. Jansen, *Z. Anorg. Allg. Chem.* **1995**, *621*, 201–206; f) C. Röhr, *Z. Kristallogr.* **1995**, *210*, 781; g) J.-T. Zhao, Z.-C. Dong, J. T. Vaughey, J. E. Ostenson, J. D. Corbett, *J. Alloys Compd.* **1995**, *230*, 1–12; h) B. Huang, J. D. Corbett, *Z.*

Anorg. Allg. Chem. **1998**, *624*, 1787–1790; i) A. Velden, M. Jansen, *Z. Anorg. Allg. Chem.* **2004**, *630*, 234–238; j) M. Kirchner, W. Schnelle, R. Niewa, *Z. Anorg. Allg. Chem.* **2006**, *632*, 559–564; k) R. Niewa, *Z. Anorg. Allg. Chem.* **2013**, *639*, 1699–1715.

[5] a) J. N. Hausmann, M. Oudah, A. Ikeda, S. Yonezawa, Y. Maeno, *Supercond. Sci. Technol.* **2018**, *31*, 055012; b) A. W. Rost, J. Kim, S. Suetsugu, V. Abdolazimi, K. Hayama, J. A. N. Bruin, C. Mühle, K. Kitagawa, A. Yarseko, J. Nuss, H. Takagi, *APL Mater.* **2019**, *7*, 121114; c) J.-H. Pöhls, A. Mar, *J. Appl. Phys.* **2019**, *126*, 025110; d) M. Bilal, S. M. Alay-e-Abbas, M. Sluydts, J. Batool, A. Laref, G. Abbas, N. Amin, *Phys. Lett. A* **2021**, *408*, 127469.

[6] a) B. Eisenmann, H. Limartha, H. Schäfer, H. A. Graf, *Z. Naturforsch.* **1980**, *B35*, 1518–1523; b) C. Hadenfeldt, H. O. Vollert, *J. Less-Common Met.* **1988**, *144*, 143–151; c) C. Hadenfeldt, H. U. Terschüren, *Z. Anorg. Allg. Chem.* **1991**, *597*, 69–78; d) J. Lin, W. Hönle, H.-G. v. Schnering, *J. Alloys Compd.* **1992**, *178*, 455–465; e) C. Feldmann, M. Jansen, *Angew. Chem.* **1993**, *105*, 1107–1108; *Angew. Chem. Int. Ed.* **1993**, *32*, 1049–1050; f) M. Asbrand, B. Eisenmann, *Z. Anorg. Allg. Chem.* **1994**, *620*, 1837–1843; g) D. Johrendt, A. Mewis, *J. Alloys Compd.* **1994**, *205*, 183–190; h) H.-G. v. Schnering, U. Bolle, J. Curda, K. Peters, W. Carillo-Cabrera, M. Somer, M. Schultheiss, U. Wedig, *Angew. Chem. Int. Ed.* **1996**, *35*, 984–986; *Angew. Chem.* **1996**, *108*, 1062–1064; i) C. Röhr, *Z. Naturforsch.* **1995**, *B50*, 802–808; j) R. George, C. Röhr, *Angew. Chem.* **1996**, *107*, 2311–2312; k) C. Röhr, R. George, *Z. Kristallogr.* **1996**, *211*, 478.

[7] a) S. Hoffmann, T. F. Fässler, C. Hoch, C. Röhr, *Angew. Chem. Int. Ed.* **2001**, *40*, 4398–4400; *Angew. Chem.* **2001**, *113*, 4527–4529; b) C. Hoch, C. Röhr, *Z. Anorg. Allg. Chem.* **2002**, *628*, 1541–1548; c) G. Frisch, C. Hoch, C. Röhr, P. Zönnchen, K.-D. Becker, D. Niemeier, *Z. Anorg. Allg. Chem.* **2003**, *629*, 1661–1667.

[8] a) A. V. Mudring, J. Nuss, U. Wedig, M. Jansen, *J. Solid State Chem.* **2000**, *155*, 29–36; b) A. V. Mudring, M. Jansen, *Angew. Chem. Int. Ed.* **2000**, *39*, 3066–3067; *Angew. Chem.* **2000**, *112*, 3194–3196; c) A. V. Mudring, M. Jansen, *Z. Anorg. Allg. Chem.* **2002**, *628*, 2200; d) M. Jansen, *Chem. Soc. Rev.* **2008**, *37*, 1826–1835.

[9] a) S. J. Clarke, G. R. Kowach, F. J. DiSalvo, *Inorg. Chem.* **1996**, *35*, 7009–7012; b) D.-G. Park, Z. A. Gal, F. J. DiSalvo, *Bull. Korean Chem. Soc.* **2005**, *26*, 1543–1548; c) L. Link, R. Niewa, *Z. Anorg. Allg. Chem.* **2020**, *646*, 1105–1109.

[10] a) A. Karpov, M. Jansen, *Angew. Chem. Int. Ed.* **2005**, *44*, 7639–7643; *Angew. Chem.* **2005**, *117*, 7813–7816; b) A. Karpov, M. Jansen, *Chem. Commun.* **2006**, *16*, 1706–1708; c) U. Wedig, V. Saltykov, J. Nuss, M. Jansen, *J. Am. Chem. Soc.* **2010**, *35*, 12458–12463; d) V. Saltykov, J. Nuss, U. Wedig, M. Jansen, *Z. Anorg. Allg. Chem.* **2011**, *637*, 357–361; e) F. Wang, U. Wedig, D. L. V. K. Prasad, M. Jansen, *J. Am. Chem. Soc.* **2012**, *134*, 19884–19894.

[11] a) A. Helms, W. Klemm, *Z. Anorg. Allg. Chem.* **1939**, *242*, 33–40; b) K.-R. Tsai, P. M. Harris, E. N. Lassettre, *J. Phys. Chem.* **1956**, *60*, 338–344; c) R. Hoppe, H. J. Röhrborn, *Z. Anorg. Allg. Chem.* **1965**, *329*, 110–122.

[12] N. J. Calos, C. H. L. Kennard, R. L. Davis, *Z. Kristallogr.* **1989**, *187*, 305–307.

[13] a) J. W. Nelson, N. C. Baenziger, *Acta Crystallogr.* **1954**, *7*, 277–282; b) E. J. Duwell, N. C. Baenziger, *Acta Crystallogr.* **1955**, *8*, 705–710; c) H. J. Deiseroth, A. Strunck, *Angew. Chem. Int. Ed.* **1987**, *26*, 687–688; *Angew. Chem.* **1987**, *99*, 701–702; d) H. J. Deiseroth, A. Strunck, *Angew. Chem. Int. Ed.* **1989**, *28*, 1251–1252; *Angew. Chem.* **1989**, *101*, 1286–1287; e) H. J. Deiseroth, A. Strunck, W. Bauhofer, *Z. Anorg. Allg. Chem.* **1989**, *575*, 31–38; f) A. V. Tkachuk, A. Mar, *Acta Crystallogr.* **2006**, *62*, i129–i130.

[14] a) L. M. Gelato, E. Parthé, *J. Appl. Crystallogr.* **1987**, *20*, 139–143; b) G. M. Sheldrick, *Acta Crystallogr.* **2008**, *A64*, 112–122; c) SADABS V. 2.03, Bruker ACS Inc. (Madison, USA), **2018**.

[15] a) G. Bergerhoff, M. Berndt, K. Brandenburg, T. Degen, *Acta Crystallogr.* **1999**, *B55*, 147–156; b) G. de la Flor, D. Orobengoa, E. Tasci, J. M. Perez-Mato, M. I. Aroyo, *J. Appl. Crystallogr.* **2016**, *49*, 653–664.

[16] A. Karpow, J. Nuss, U. Wedig, M. Jansen, *Angew. Chem. Int. Ed.* **2003**, *42*, 4818–4821; *Angew. Chem.* **2003**, *115*, 4966–4969; M. Jansen, *Solid State Sci.* **2005**, *7*, 1464–1474; M. Jansen, *Chem. Soc. Rev.* **2008**, *37*, 1824–1835.

[17] J. Weidlein, U. Müller, K. Dehnicke, *Schwingungsspektroskopie – Eine Einführung, 2nd Ed.*, **1988**, Thieme, Stuttgart, New York.

[18] C. Hoch, C. Röhr, *Z. Naturforsch.* **2001**, *56*, 1245–1256.

[19] a) J. P. Perdew, K. Burke, M. Ernzerhof, *Phys. Rev. Lett.* **1996**, *77*, 3865–3868; b) J. P. Perdew, K. Burke, M. Ernzerhof, *Phys. Rev. Lett.* **1997**, *78*, 1396; c) P. Blaha, K. Schwarz, G. K. H. Madsen, D. Kvasnicka, J. Luitz, TU Wien (Wien. Austria), **2006**.

Manuscript received: December 22, 2021
Revised manuscript received: January 24, 2022
Accepted manuscript online: February 1, 2022

